Supramolecular hybrid of Fe pentanuclear complex/ diblock copolypeptide amphiphiles with pH-responsive nano/microstructures in water.

Keita Kuroiwa‡, Touka Tada,‡ Miki Ichise,‡ Shigeyuki Masaoka.†*

‡ Department of Nanoscience, Faculty of Engineering, Sojo University, 4-22-1 Ikeda, Nishi-ku, Kumamoto 860-0082, Japan

† Division of Applied Chemistry, Graduate School of Engineering, Osaka University, 2-1 Yamadaoka, Suita, Osaka 565-0871, Japan.

Keywords: Self-assembly, Nanohybrid, Diblock Copolypeptide Amphiphiles, Fe pentanuclear complex, Electrochemical Oxidation.

Table of Contents

1. General polypeptide synthesis

All diblock copolypeptide amphiphiles were synthesized using $Co(PMe_3)_4$ as the initiator and following a literature procedure (Fig. S1) [1]. Briefly, in each synthesis, a 50 mL glass vial was charged with 1 g of the *N*-carboxyanhydride (NCA) of β-benzyl-L-aspartate (Bzl-L-Asp) and 20 ml of tetrahydrofuran (THF), after which this mixture was stirred in a glove box. The required amount of $Co(PMe_3)_4$ and 2.0 mL of THF was then transferred to a 20 ml glass vial, after which 1.2 mL of the $Co(PMe_3)_4$/THF solution was transferred to the NCA/THF solution in the 50 mL vial by syringe and the mixture was stirred for 2 h. The polymerization degree was four times the ratio of the total moles of NCA monomers (L-Asp + L-Leu) to the moles of $Co(PMe_3)_4$ [2,3]. Following this, the product was characterized by FTIR spectroscopy and GPC.

A 20 mL glass vial was then charged with a variable amount of the NCA of L-Leu and 0.5 ml of dry THF. The contents of the vial were subsequently transferred into a 50 ml glass vial containing the $Co(PMe_3)_4$/Bzl-L-Asp/THF solution and stirred overnight. The resulting product was a Bzl-L-Asp-*block*-L-Leu copolypeptide. This material was also analyzed using FTIR spectroscopy. The Bzl-L-Asp-*block*-L-Leu was subsequently transferred to a 100 mL flask and the residual solvent was removed under vacuum. Following this, 100 mL of dichloromethane (DCM) was added to the copolypeptide together with 3.0 mL of TMSI, and the mixture was heated to 40 °C with stirring for 12 h. After cooling the solution, 50 mL of hexane and 50 mL of deionized water were added to the mixture, following which the precipitated solid phase was removed by filtration and washed with hexane and acetone then dried overnight. The resulting solid was dispersed in a 0.1 M aqueous NaOH solution and the sediment was transferred to a dialysis tube, after which a dialysis procedure was carried out for one week. During the first two days of this process, the tube was placed in 2.0 L of a 0.10 M aqueous EDTA solution that was

replaced daily. Over the next three days, the tube was placed in 2.0 L of a 0.10 M aqueous NaCl solution, with daily replacement of the solution. Finally, during the last two days, the tube was placed in 2.0 L of deionized water, with daily replacement of the deionized water. The sediment in the tube dissolved in water and changed to a transparent solution, although salting out occurred during the EDTA and NaCl process. Following dialysis, the solution was transferred to a centrifuge tube and freeze dried to yield 50 mg of a colorless powder. The degree of polymerization, polydispersity, composition and proportion of Bzl-L-Asp **units** in each of these copolypeptides were determined using GPC (Table S1), ^{1}H NMR spectroscopy with a 400 MHz instrument (Figs. S2 – S7) and FTIR spectroscopy (Figs. S8 – S13).

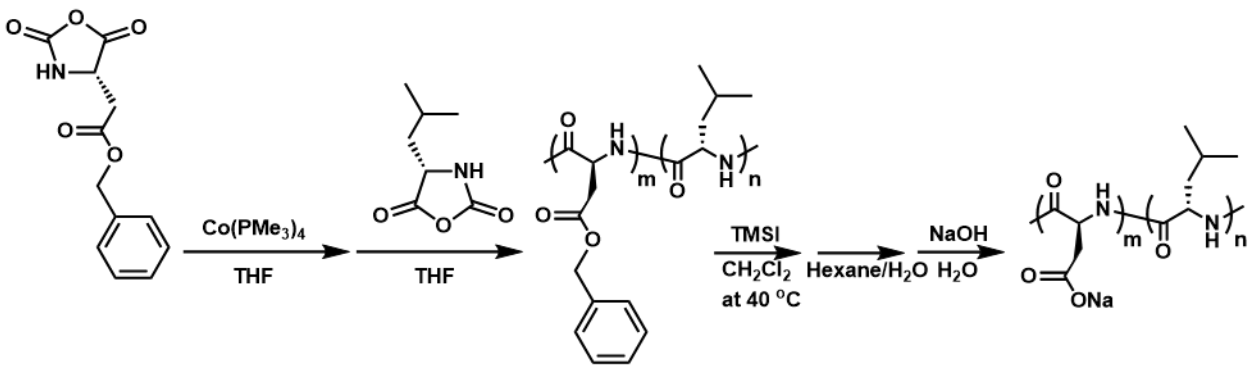

Figure S1. The procedure used to synthesize diblock copolypeptide amphiphiles **1** – **6**.

Table S1. Properties of the diblock copolypeptide amphiphiles synthesized in this work.

Polypeptides	M_n [a]	M_w/M_n [a,b]	Asp_m length [c]	Found composition [d]
1	2.36 x 10^4	1.02	$(Bzl\text{-}Asp)_{114}$	$(Asp)_{114}$-*b*-$(Leu)_6$
2	3.34 x 10^4	1.09	$(Bzl\text{-}Asp)_{163}$	$(Asp)_{163}$-*b*-$(Leu)_9$
3	4.27 x 10^4	1.02	$(Bzl\text{-}Asp)_{208}$	$(Asp)_{208}$-*b*-$(Leu)_{41}$

a Determined using gel permeation chromatography based on unprotected Bzl-Asp units.
b M_w/M_n = Polydispersity index.
c Determined from Mn measurements (GPC).
d Determined from Mn measurements and ^{1}H NMR analysis of deprotected samples.

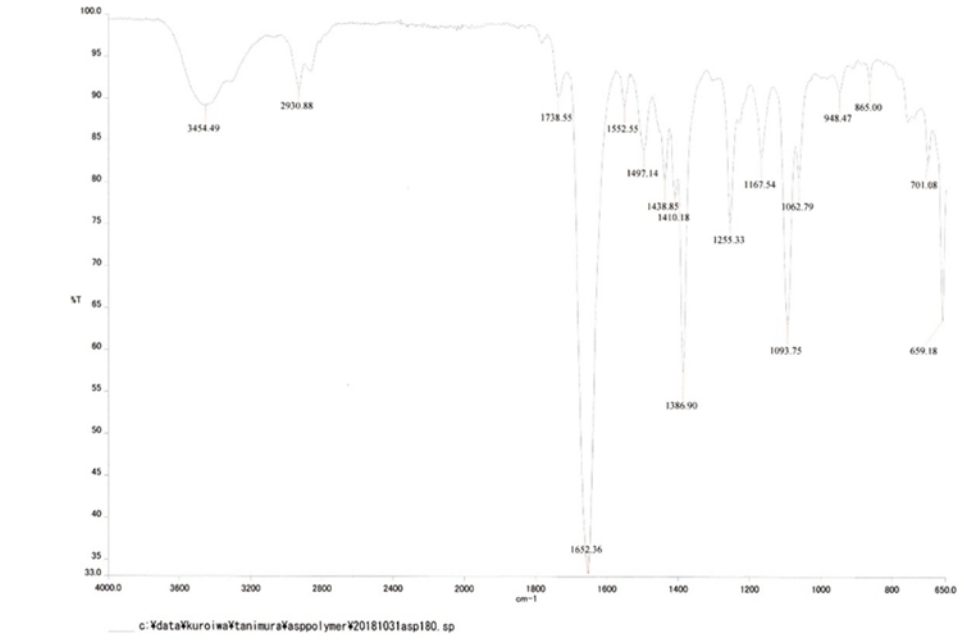

Figure S2. ATR FTIR spectrum of Asp$_{114}$-*b*-Leu$_6$ (**1**).

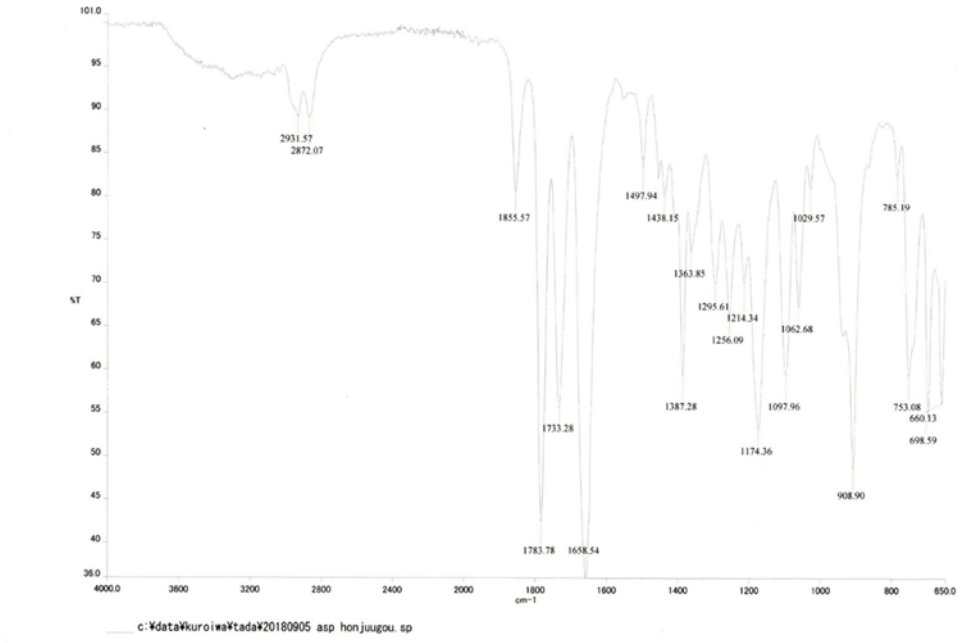

Figure S3. ATR FTIR spectrum of Asp$_{163}$-*b*-Leu$_9$ (**2**).

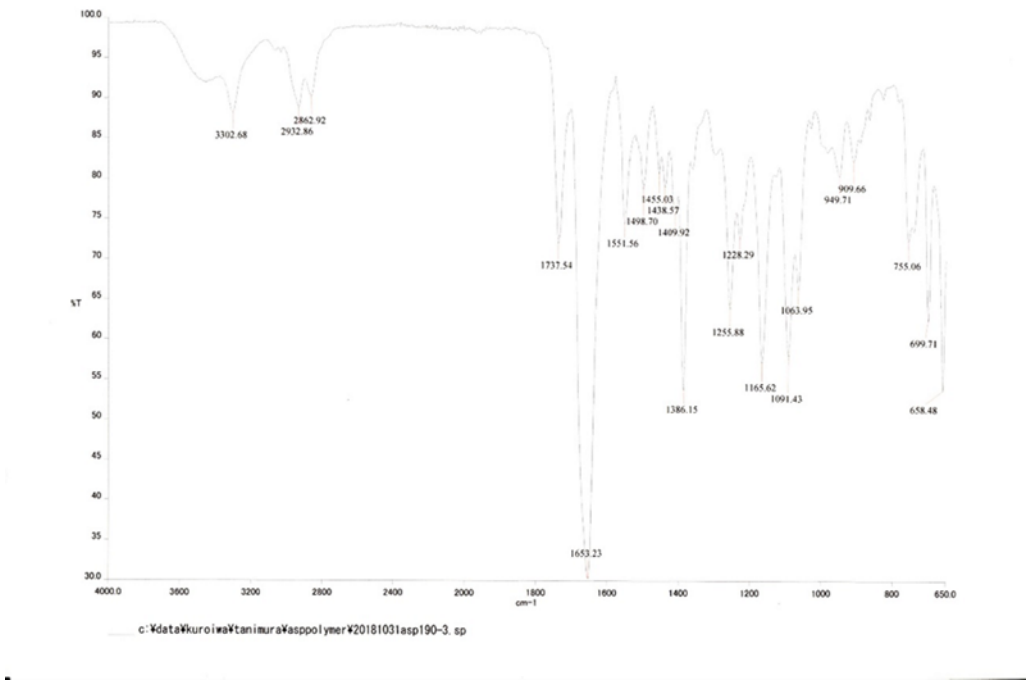

Figure S4. ATR FTIR spectrum of Asp_{208}-*b*-Leu_{41} (**3**).

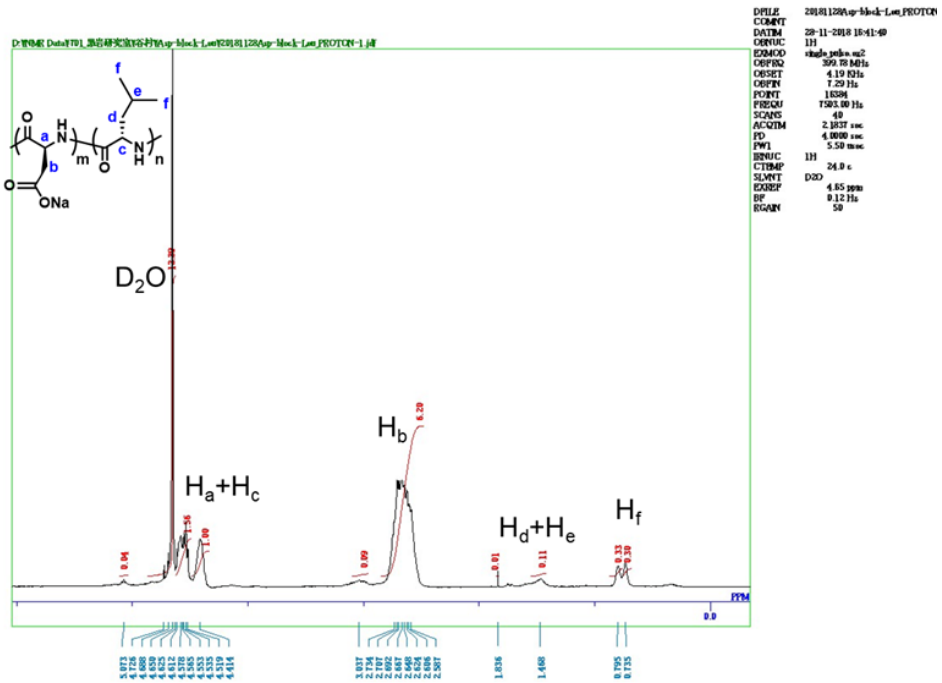

Figure S5. ^{1}H NMR spectrum of Asp_{114}-*b*-Leu_6 (**1**) (400 MHz, D_2O, r.t.).

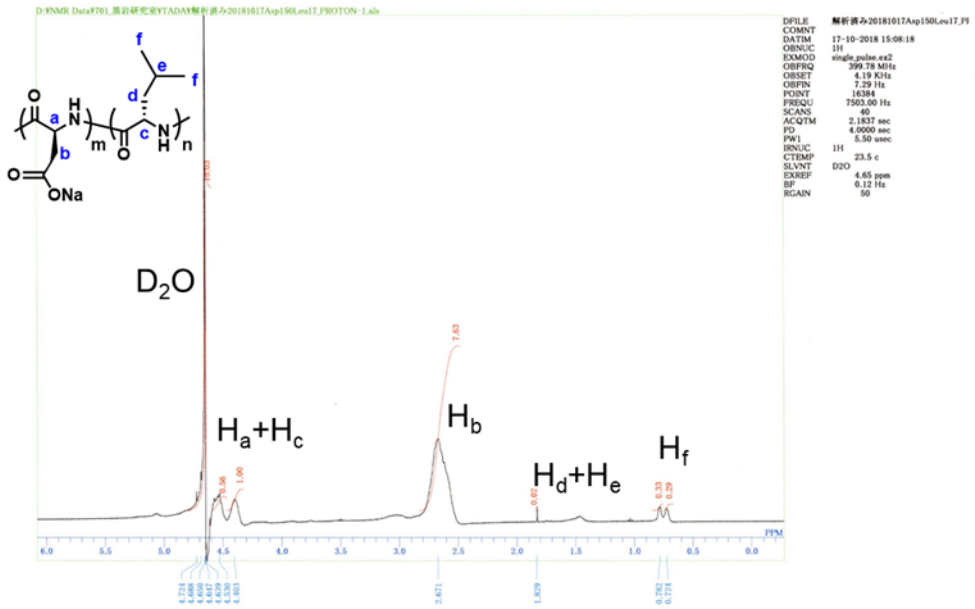

Figure S6. ^{1}H NMR spectrum of Asp$_{163}$-*b*-Leu$_{9}$ (**2**) (400 MHz, D_2O, r.t.).

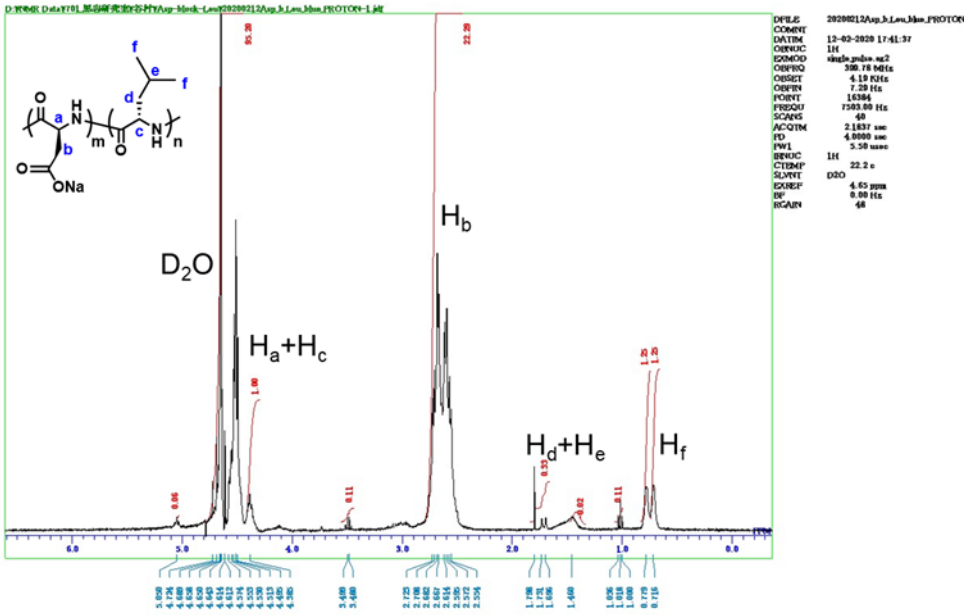

Figure S7. ^{1}H NMR spectrum of Asp$_{208}$-*b*-Leu$_{41}$ (**3**) (400 MHz, D_2O, r.t.).

2. General preparation of $Na_x(Asp_m$-*b*-$Leu_n)_y[Fe^{II}_4Fe^{III}(\mu_3\text{-}O)(\mu\text{-}L)_6]^{3+}{}_z$ (Fe5; LH = 3,5-bis(2-pyridyl)pyrazole)

A quantity of $Na_m(Asp_m$-*b*-$Leu_n)$ equivalent to 9 μmol Asp was dissolved in 10 ml of deionized water. The hybrid $Na_x(Asp_m$-*b*-$Leu_n)_y$[**Fe5**]$_z$ was subsequently prepared by combining 4 ml of this $Na_m(Asp_m$-*b*-$Leu_n)$ aqueous solution with 2.7 μmol of [**Fe5**]$(BF_4)_3\cdot 7H_2O$ to obtain a metal complex concentration of 0.27 mM and a Asp : [**Fe5**] molar ratio of 10 : 3. This ratio was selected based on prior optimization studies showing that a 10 : 3 proportion affords the highest solubility and most stable dispersion of the hybrid complex in water. This mixture was stirred for one week then transferred to a dialysis tube after which a dialysis procedure was carried out for two days. Throughout this time period the tube was placed in 2.0 L of deionized water with daily replacement of the deionized water, during which time the sediment of metal complex in the tube dissolve in water, and changed to a transparent solution, although the metal complex did not dissolve in water. The dialyzed solution was then transferred to a centrifuge tube and freeze dried to yield a pale brown powder. The proportions of Fe in the material were determined using ICP-OES (Table S2).

Hybrid 1: Yield 9.8 mg $Na_{12}(Asp_{114}$-*b*-$Leu_6)$[**Fe5**]$_{34}$

Elemental analysis: Found (%): C, 53.65; H, 3.58; N, 18.63.

Calc. (%) for $C_{3144}H_{2358}Fe_{170}N_{936}Na_{12}O_{382}$: C, 54.62; H, 3.44; N, 18.96.

Hybrid 2: Yield 8.3 mg $Na_{16}(Asp_{163}$-*b*-$Leu_9)$[**Fe5**]$_{49}$

Elemental analysis: Found (%): C, 53.80; H, 3.59; N, 18.69.

Calc. (%) for $C_{4528}H_{3397}Fe_{245}N_{1348}Na_{16}O_{547}$: C, 54.86; H, 3.61; N, 18.79.

Hybrid 3: Yield 9.6 mg $Na_{22}(Asp_{208}$-*b*-$Leu_{41})$[**Fe5**]$_{62}$

Elemental analysis: Found (%): C, 53.92; H, 3.78; N, 18.42.

Calc. (%) for $C_{5914}H_{4631}Fe_{310}N_{1737}Na_{22}O_{727}$: C, 54.86; H, 3.61; N, 18.79.

Table S2. Fe concentrations as determined by ICP-OES in hybrids **1** – **3** (mg/L), using an approximately 1.00 mg/L sample in each case.

Hybrid	Fe	
	Found (mg/L)	Calc. (mg/L)
1 /[**Fe5**]	1.027	1.030
2 /[**Fe5**]	1.011	1.020
3 /[**Fe5**]	1.046	1.050

3. SEM observations of hybrids

Scanning electron microscopy (SEM) was carried out with an ERA-600 microscopy (Elionix Inc. Tokyo, Japan). operating at 20 kV. Scanning electron microscope samples were prepared by transferring the surface layers of dispersions to Cu plate.

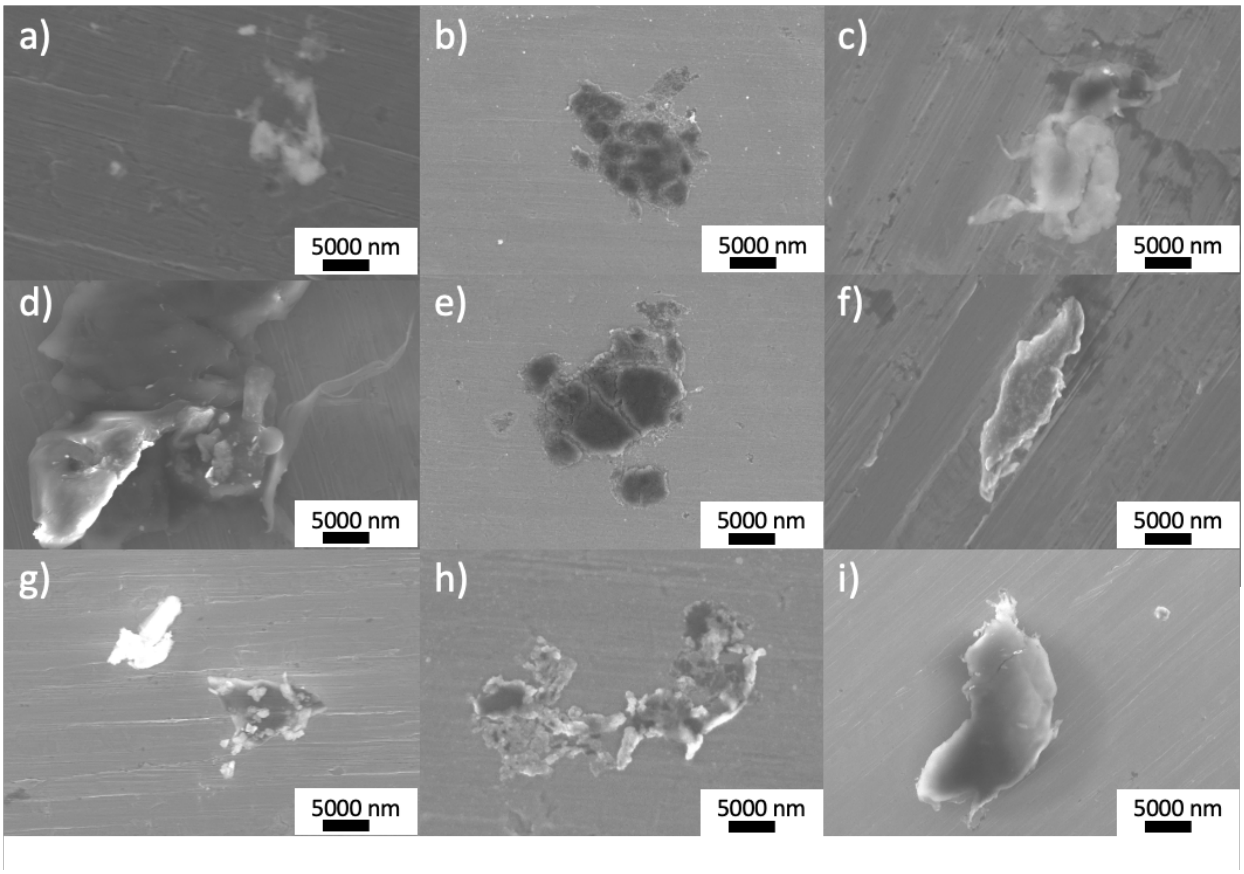

Figure S8. SEM images of (a) 1 /Fe5 at pH 4, (b) 1 /Fe5 at pH 7, (c) 1 /Fe5 at pH 10, (d) 2 /Fe5 at pH 4, (e) 2 /Fe5 at pH 7, (f) 2 /Fe5 at pH 10, (g) 3 /Fe5 at pH 4, (h) 3 /Fe5 at pH 7, (i) 3 /Fe5 at pH 10, where [Fe5 complex] =0.1 mg/mL.

4. Scanning transmission electron microscopy coupled with energy dispersive X-ray spectroscopy (HR-STEM EDX) measurement

High-resolution scanning transmission electron microscopy coupled with energy dispersive X-ray spectroscopy (HR-STEM EDX) was performed using a Titan Themis 200 (Thermo Fisher Scientific Co. Ltd., Waltham, MA, USA) operating at 200 kV. Transmission electron microscope samples were prepared by transferring the surface layers of dispersions to carbon-coated Cu TEM grids.

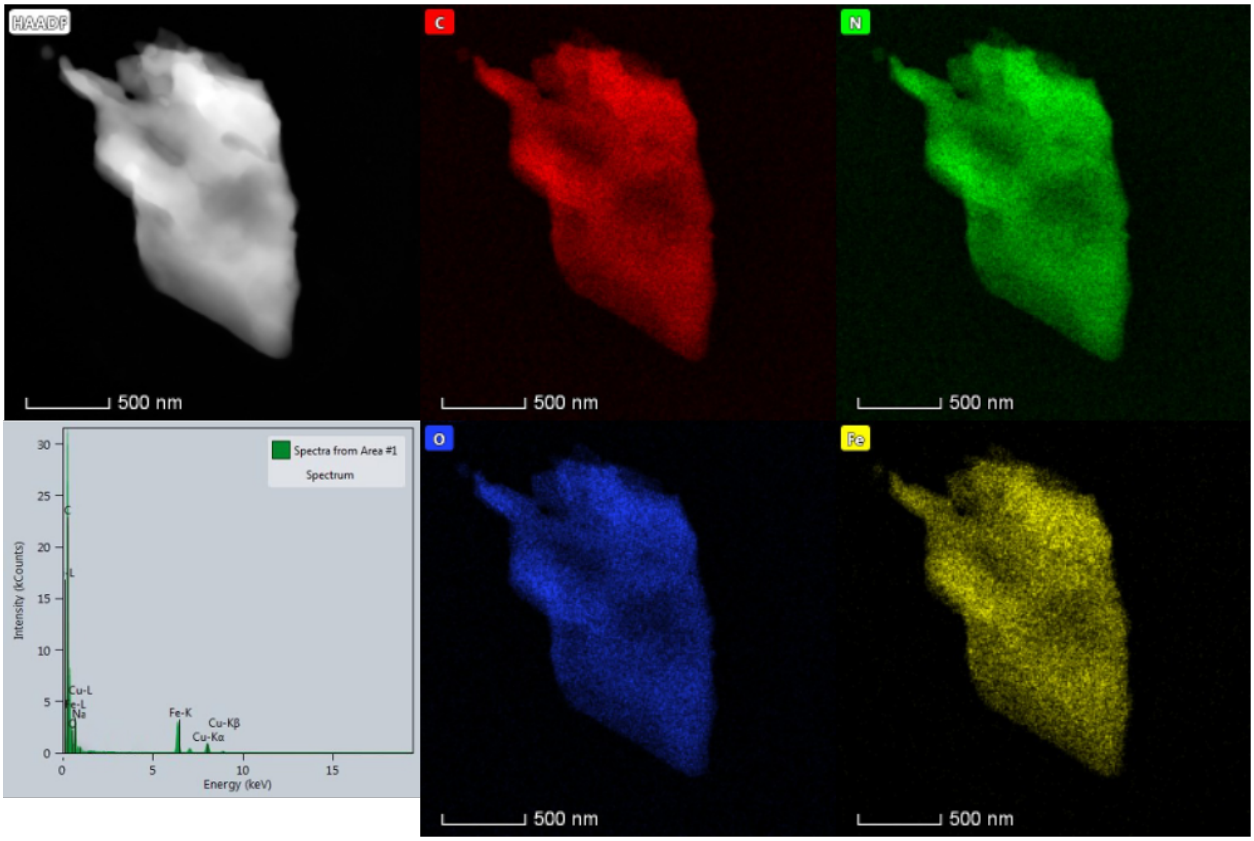

Figure S9. HAADF-STEM image and STEM-EDX maps within the HAADF-STEM of **1**/ [**Fe5**] at pH 7, where [Fe complex] =0.1 mM.

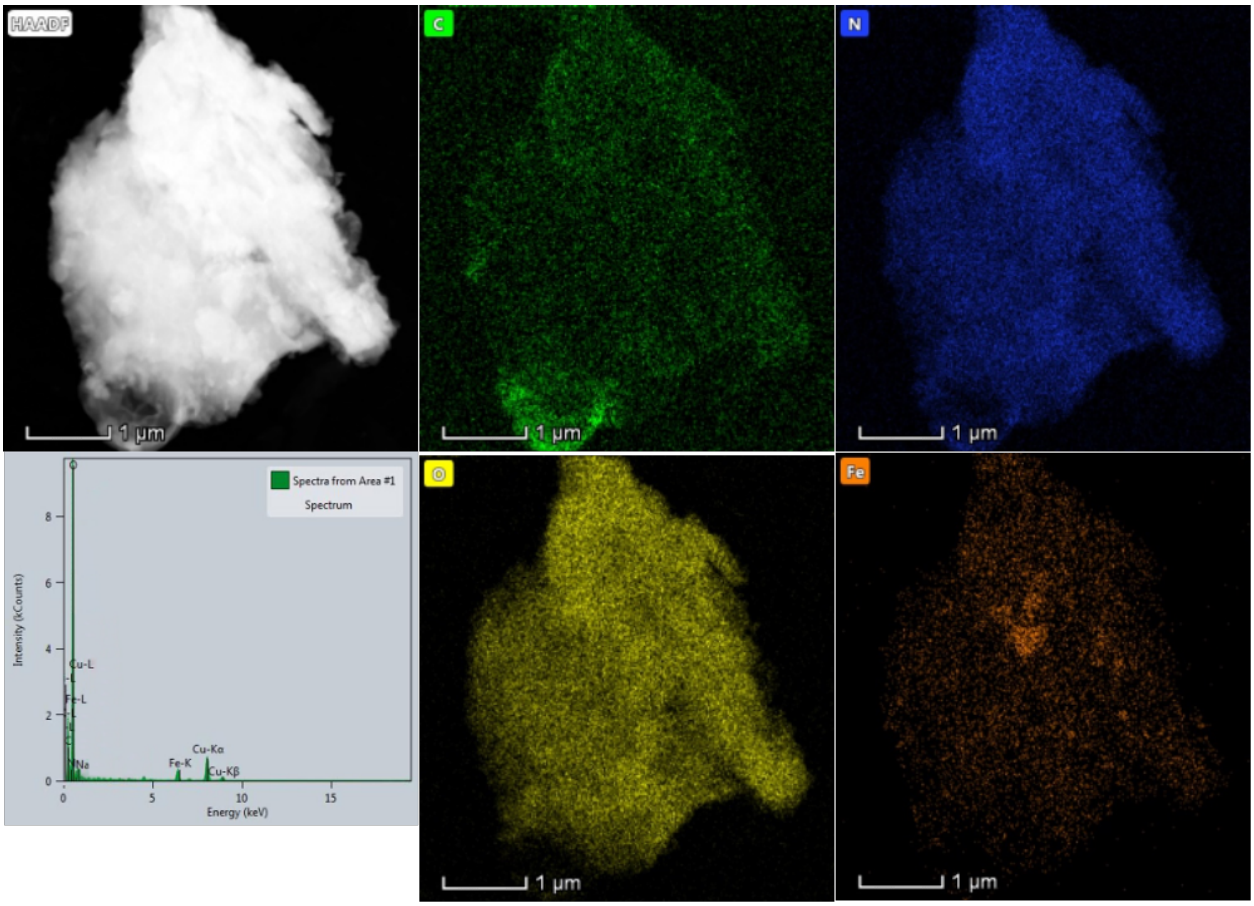

Figure S10. HAADF-STEM image and STEM-EDX maps within the HAADF-STEM of **2**/ [**Fe5**] at pH 7, where [Fe complex] =0.1 mM.

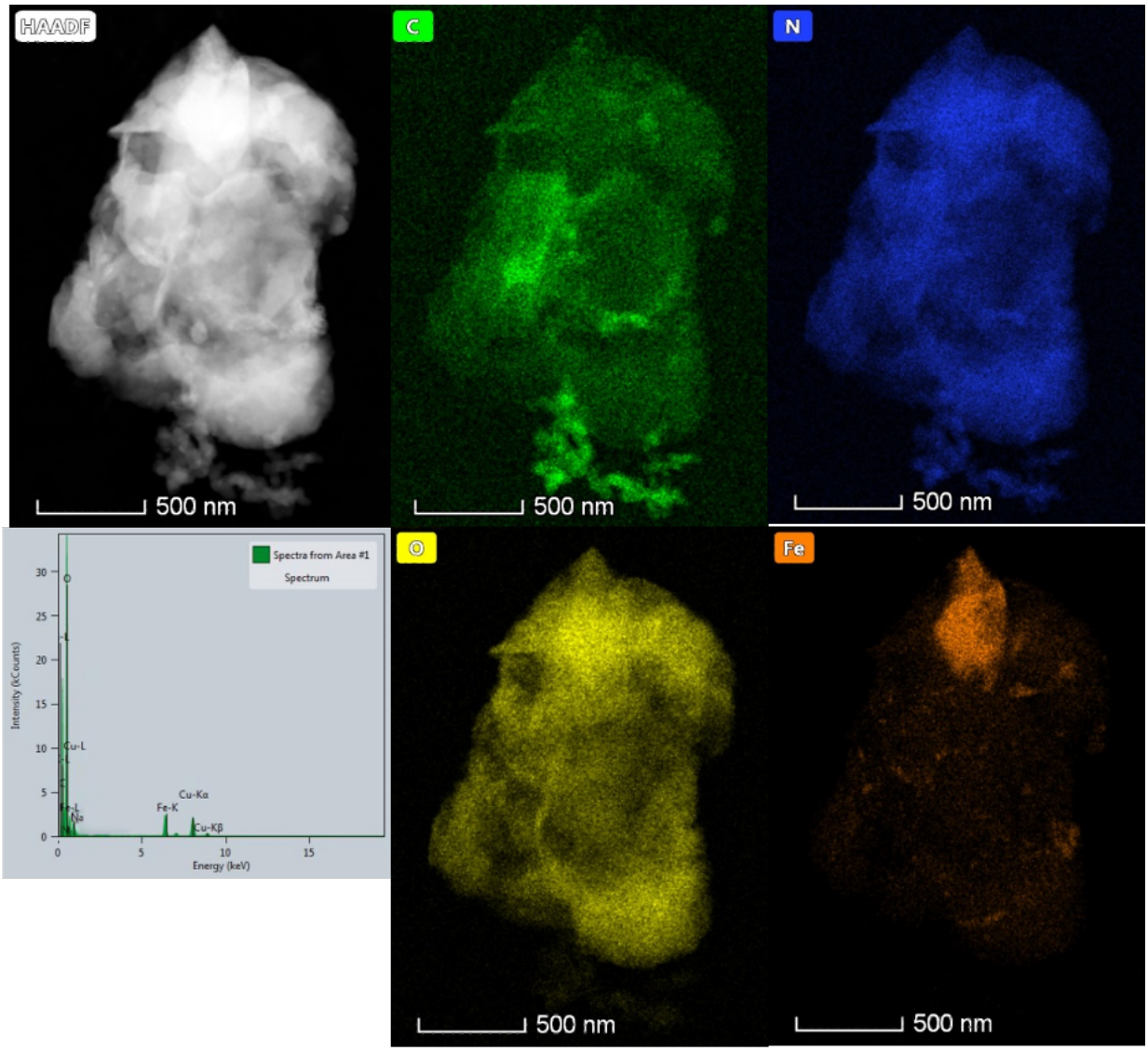

Figure S11. HAADF-STEM image and STEM-EDX maps within the HAADF-STEM of **3**/ [**Fe5**] at pH 7, where [Fe complex] =0.1 mM.

5. AlphaFold2 simulation of the diblock copolypeptide amphiphile

The diblock copolypeptide was modeled using AlphaFold2 [4, 5]. The amino-acid sequence of Polypeptide 1 was submitted as input, and structure prediction was performed using the automated AlphaFold2 pipeline. The resulting structural model was visualized using PyMOL. It should be noted that the simulation was conducted for a single polypeptide chain; therefore, intermolecular interactions between multiple peptide molecules were not considered.

The predicted structure suggests that the aspartic-acid–rich segment preferentially adopts β-sheet and random-coil–like conformations, whereas the leucine segment has a strong propensity to form α-helical structures. These features are consistent with the secondary-structure information obtained from the CD spectra. Furthermore, closer inspection of the isolated aspartic-acid segment reveals that the side-chain carboxylate groups are arranged with slight torsional deviations, forming a spatial orientation that is likely favorable for interaction with the **Fe5** complex.

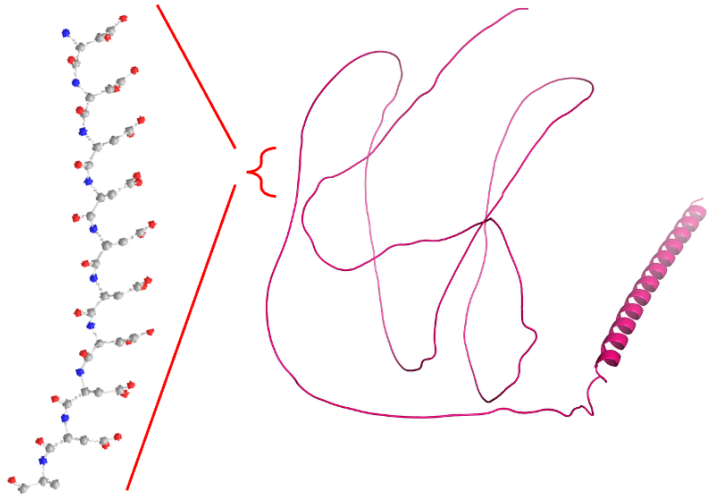

Figure S12. AlphaFold2 simulation of the diblock copolypeptide amphiphile (**3**). The left panel shows a magnified view of the aspartic-acid segment, and the right panel presents the predicted overall three-dimensional structure. The simulation was performed for a single polypeptide molecule; therefore, intermolecular interactions were not taken into account.

REFERENCES

1. Tanimura, Y.; Sakuragi, M.; Deming, T. J.; Kuroiwa, K. Self-Assembly of Soluble Nanoarchitecture using Hybrids of Diblock Copolypeptide Amphiphiles with Copper Rubeanate Hybrates in Water and Their Elecctrooxidation Reaction. *ChemNanoMat* **2020**, *6*, 1635–1640.
2. Pochan, D.J.; Pakstis, L.; Ozbas, B.; Nowak, A.P.; Deming, T.J. SANS and cryo-TEM Study of Self-assembled Diblock Copolypeptide Hydrogels with Rich Nano-through Microscale Morphology. *Macromolecules* **2002**, *35*, 5358–5360.
3. Novak, A.P.; Breedveld, V.; Pakstis, L.; Ozbas, B.; Pine, D.J.; Pochan, D.; Deming, T.J. Rapidly Recovering Hydrogel Scaffolds from Self-assembling Diblock Copolypeptide Amphiphiles. *Nature* **2002**, *417*, 424–428.
4. Jumper, J.; Evans, R.; Pritzel, A.; Green, T.; Figurnov, M.; Ronneberger, O.; Tunyasuvunakool, K.; Bates, R.; Zidek, A.; Potapenko, A.; et al. Highly accurate protein structure prediction with AlphaFold. *Nature* **2021**, *596* (7873), 583–589.
5. Varadi, M.; Anyango, S.; Deshpande, M.; Nair, S.; Natassia, C.; Yordanova, G.; Yuan, D.; Stroe, O.; Wood, G.; Laydon, A.; et al. AlphaFold Protein Structure Database: massively expanding the structural coverage of protein-sequence space with high-accuracy models. *Nucleic Acids Res.* **2022**, *50* (D1), D439–D444.